Modeling Of A Diffraction Grating Coupled Waveguide Based Biosensor For Microfluidic Applications

Y. Wu[1], M. L. Adams[1]
[1]Auburn University, Department of Electrical and Computer Engineering, Auburn, AL, USA

Introduction:

Grating couplers are a common optical component for introducing light into chip-based photonic structures. They are used extensively for optical interconnects and optical device integration. A microfluidic diffraction grating coupled waveguide (MDGCW) biosensor applies a grating coupler for label-free detection of a biological analyte. A novel MDGCW is modeled and the results presented. The results illustrate the high sensitivity of the biosensor for measuring the refractive index of the binding layer.

Computational Methods:

The boundary mode analysis is used to run the simulation and is solved for the propagation constant.

$$\nabla \times \mu_r^{-1}(\nabla \times E) - k_0^2\left(\epsilon_r - \frac{j\sigma}{\omega\epsilon_0}\right)E = 0$$

$$\lambda = -j\beta - \delta_z$$

$$E(x,y,z) = \tilde{E}(x,y)e^{-ik_z z}$$

The sensor is composed of the optical elements, a flow cell with medium, and a binding layer that is formed on the dielectric slab of optical elements.

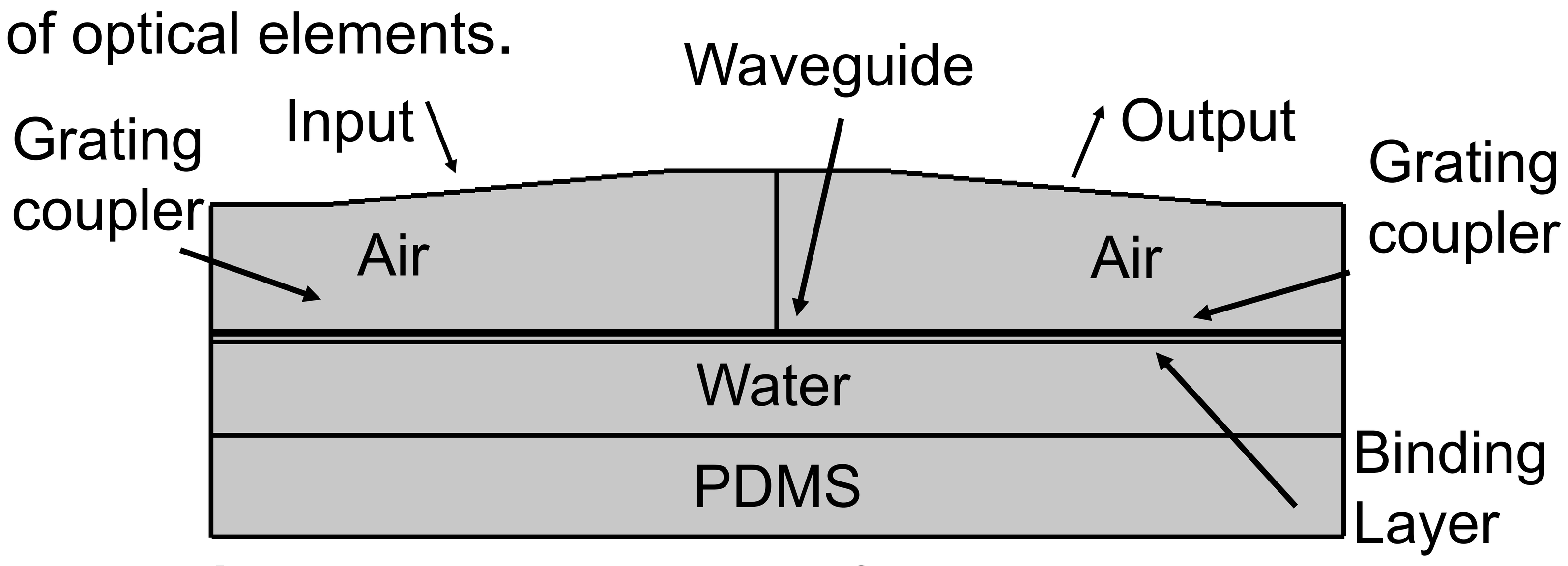

Figure 1. The geometry of the sensor

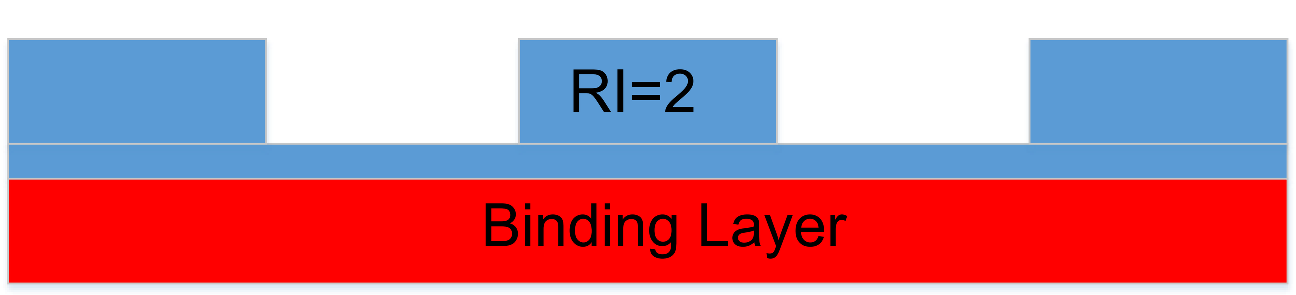

Figure 2. The detail of the sensor and the binding layer

$$n_{eff} = n_{top} * sin\varphi_i + m\frac{\lambda}{d}$$

$$\Delta n_{eff} = n_{top} * sin\varphi_i + m\frac{\Delta\lambda}{d}, \quad S = \frac{\Delta\lambda}{\Delta n}$$

Factors that affect the n_{eff} : dimensions of the structure and the refractive index of the media.

Factors that affect the $\Delta\lambda$: Δn_{eff}, d, n_{top}, $sin\varphi_i$.

The binding layer is modeled to detect the refractive index. For different refractive indices or different coupling angles, the propagation mode of the light coupled in the grating waveguide will be changed, causing the shift of the peak in the spectrum.

When the refractive index of the binding layer is changed by the analyte of interest, the peak shift will be linearly proportional to the change of the refractive index.

Results:

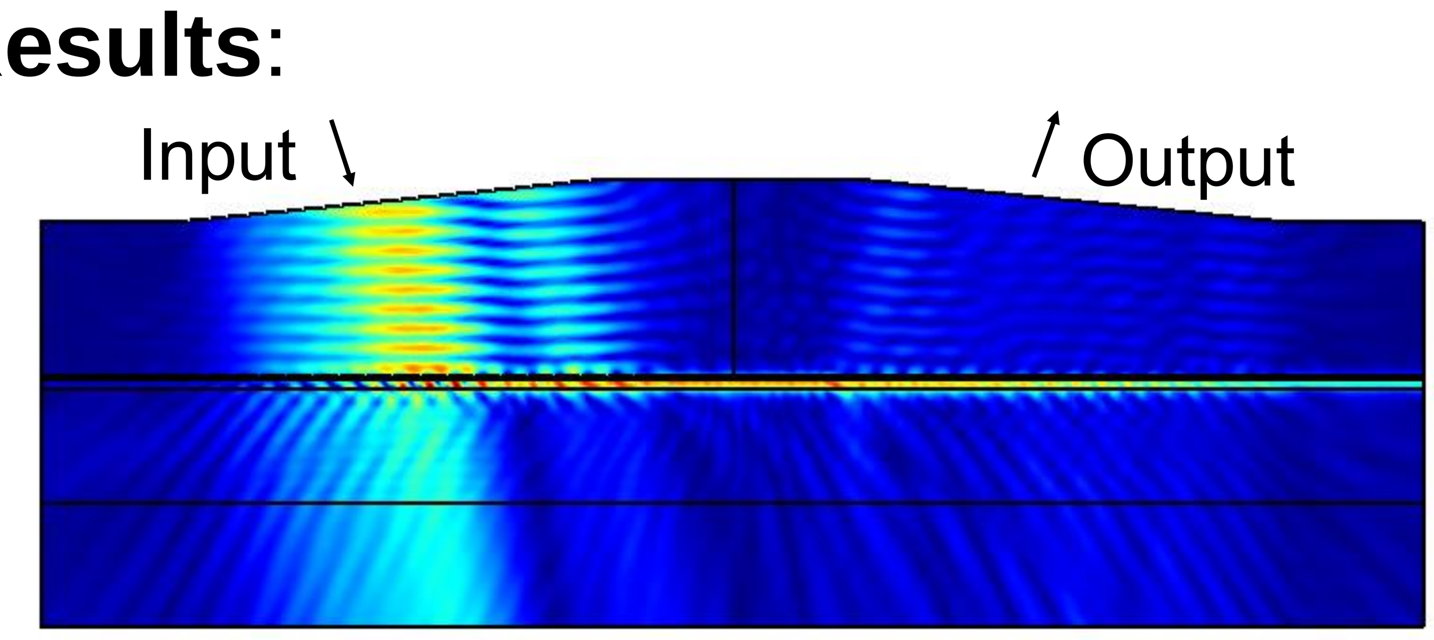

Figure 3. Electrical field distribution of the sensor

(1). Incidence angles of $5.7°$, $7.9°$ and $10.1°$ are shown as Figures 4, 5 and 6, respectively.
(2). Binding layer thicknesses of 0.2μm, 0.15μm and 0.1μm are shown as Figures 4, 7, and 8, respectively.
(3). A comparison of the different incident angles for n_{bl} = *1.7* is shown as Figure 9.

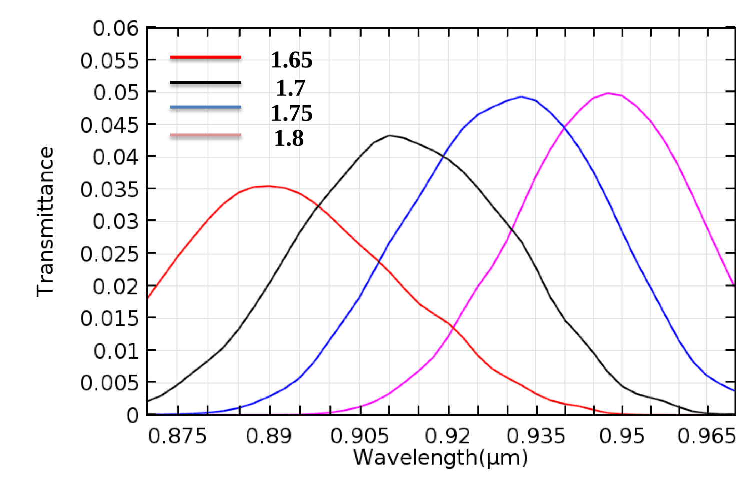

Figure 4. Spectrum when binding layer is 0.2μm and coupling angle is 5.7°

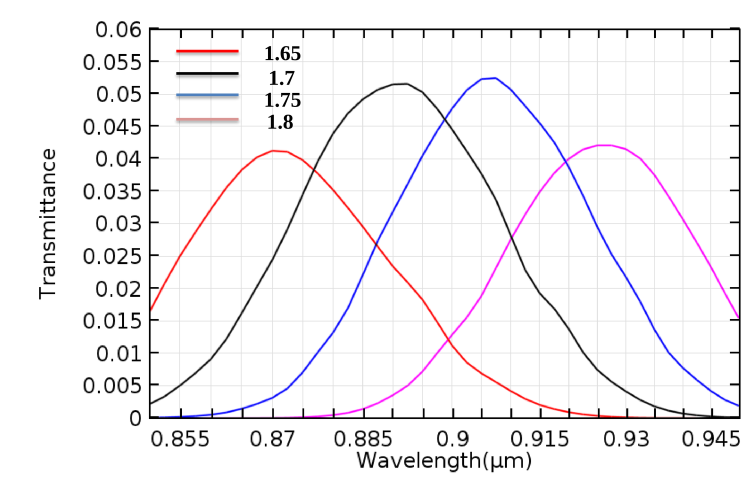

Figure 5. Spectrum when binding layer is 0.2μm and coupling angle is 7.9°

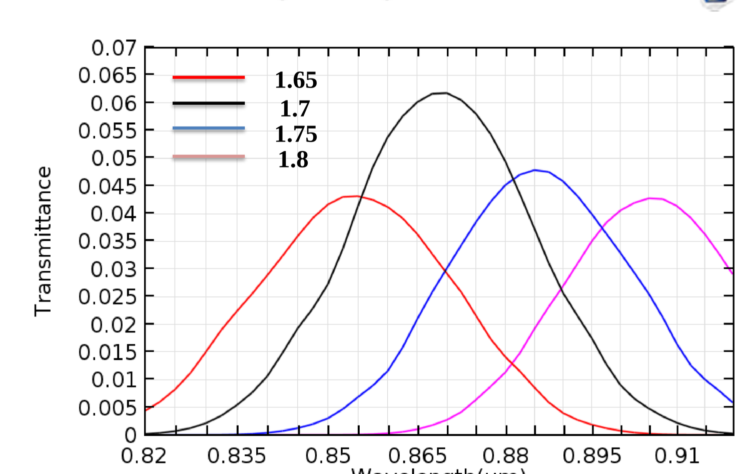

Figure 6. Spectrum when binding layer is 0.2μm and coupling angle is 10.1°

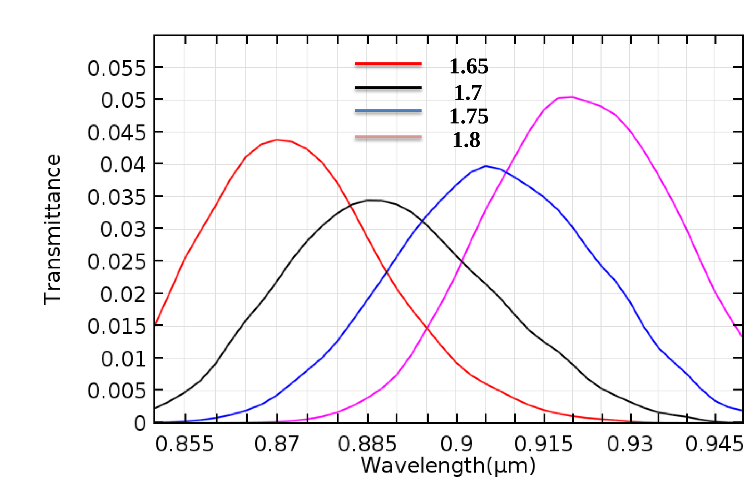

Figure 7. Spectrum when binding layer is 0.15μm and coupling angle is 5.7°

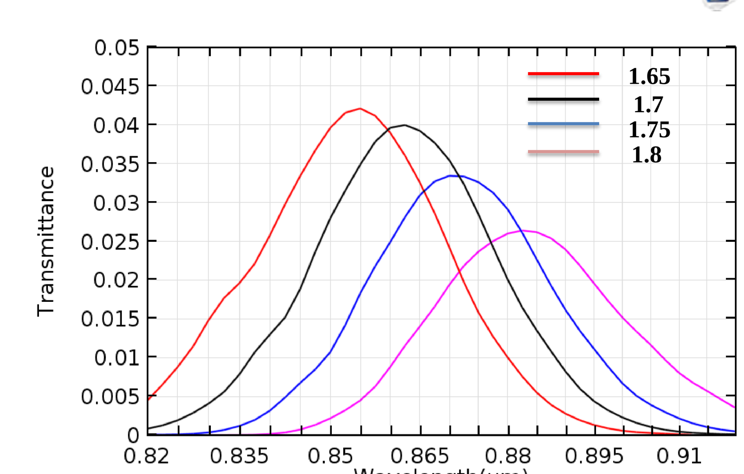

Figure 8. Spectrum when binding layer is 0.1μm and coupling angle is 5.7°

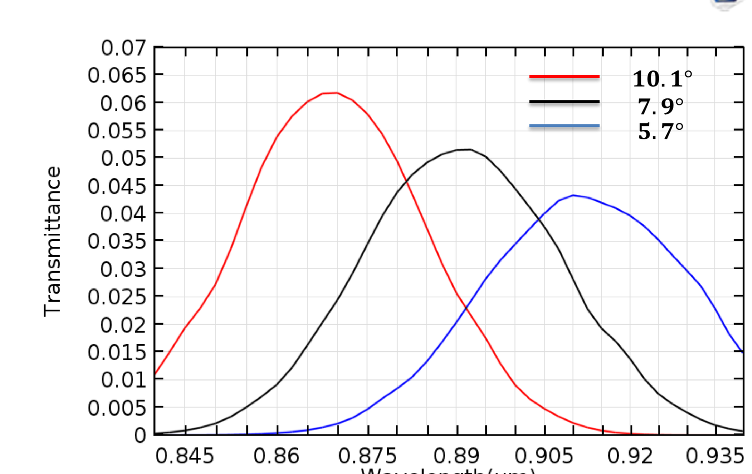

Figure 9. Spectrum when binding layer is 0.2μm and the refractive index of the binding layer is 1.7

Conclusions:

Good sensitivity of the biosensor is obtained by the simulation. From the results, the refractive index of the binding layer, the dimension of the binding layer, and the coupling angle will affect the sensitivity. Furthermore, since the effective mode index of the grating is related to the grating period, the thickness of the grating, and the etch depth of the grating, changes to any of these parameters allow further optimization of the MDGCW based biosensor.

Reference:

1. H. Mukundan et al., Waveguide-Based Biosensors for Pathogen Detection, Sensors, 9, 5783- 5809 (2009)
2. Y. Guo et al, Optofluidic Fabry–Pérot cavity biosensor with integrated flow-through micro-/nanochannels, Applied Physics Letters, 98, 041104 (2011)
3. M. L. Dakss et al., Grating Coupler for Efficient Excitation of Optical Guided Waves in Thin Films," Appl. Phys.Lett, 16, 523-525 (1970)
4. N. Darwish et al., Multi-analytic grating coupler biosensor for differential binding analysis, Sensors and Actuators B, 144, 413–417 (2010)
5. D. Duval et al., Grating Couplers Integrated on Mach–Zehnder Interferometric Biosensors Operating in the Visible Range, IEEE Photonics Journal, 5, 3700108-3700108 (2013)
6. J. Vörös et al., Optical grating coupler biosensors, Biomaterials, 23, 3699-3710 (2002)
7. X. Wei and S. M. Weiss, Guided mode biosensor based on grating coupled porous silicon waveguide, Opt. Exp., 19, 11330-11339 (2011)
8. Z. Lai et al., Label-free biosensor by protein grating coupler on planar optical waveguides, Opt. Let., 33, 1735-1737 (2008)
9. P. Kozma et al., Grating coupled optical waveguide interferometer for label-free biosensing, Sen. and Act. B, 155, 446–450 (2011)

Excerpt from the Proceedings of the 2016 COMSOL Conference in Boston